UNIVERSITY OF BIRMINGHAM

Understanding the effect of metamictization on the efficiency of zircon milling

Smith, Matthew J.; Jones, Emma; Blackburn, Stuart; Greenwood, Richard W.

[Link to publication on Research at Birmingham portal](#)

Understanding the effect of metamictization on the efficiency of zircon milling

Matthew J. Smith [*], Emma Jones , Stuart Blackburn , Richard W. Greenwood

School of Chemical Engineering, University of Birmingham, Birmingham B15 2TT, UK

ARTICLE INFO

Keywords:
Metamictization
Zircon
Radiation
Milling

ABSTRACT

Six commercially available zircon sands were characterised by XRD, SEM, BET and helium pycnometry to determine their degree of metamictization. These sands were categorized into pairs denoted as high, medium or low levels of metamictization. The six samples were subsequently dry milled under identical conditions and their milling behaviour was tracked by measuring the particle size distribution at regular intervals. Samples with low levels of metamictization were found to achieve a marginally smaller particle size than samples with high levels of metamictization after prolonged milling. This was attributed to two potential mechanisms during breakdown – brittle fracture in the former due to retained hardness, in comparison to a more ductile resistance to fracture in the latter due to reduced hardness. However, no clear trend between specific metamictization characteristics and milling behaviour was found. The results reveal a poorer overall milling efficiency for high metamict samples, which has implications such as increased energy costs, poor quality product and a need for further processing of samples exhibiting high levels of metamictization. This study creates a novel link between the milling behaviour of zircon and its level of metamictization. The knowledge gained holds strong importance for industrial entities wishing to carry out and maintain an efficient milling process, with feed material quality likely to become more variable in future years.

1. Introduction

Zirconium silicate ($ZrSiO_4$), commonly known as zircon, is used as a component in many everyday products, including in ceramic tiles. It also has several large-scale industrial applications such as refractories, abrasives and foundry sands. Zircon is most commonly obtained as a bi- or co-product from the mining of ilmenite and rutile from heavy mineral sand deposits. It can be extracted during processing to provide coarse zircon sand, or it may be further processed into a finer powder known as zircon flour. With annual global extraction of zircon consistently exceeding one million tonnes (Zircon Industry Association, 2015), the majority of which is subsequently milled to a specified size, it is of great industrial interest to understand the energy use of the milling process and the required parameters for sands of varying origin. An area of particular interest is that surrounding the effect of metamictization (radiation damage) on the milling behaviour of zircon. Metamictization is known to affect several key physical properties of zircon, such as density, crystallinity and hardness.

On an industrial scale, it is important to understand how metamictization of zircon might affect the milling process such that any change in efficiency can be accounted for and, furthermore, so that any necessary method adaptation or standardisation can be implemented based on a known level of metamictization in the feed material. Additionally, it is important to understand any direct impact on product quality due to variation in physical characteristics of zircon caused by radiation. These factors are particularly important to the zircon industry, since depletion of low-metamict zircon sources will ultimately create the need to utilise material of variable quality.

The linkage of two areas of research, namely metamictization and milling performance of zircon, is not reported in the literature, to the best of the authors' knowledge. Therefore, this paper provides a useful starting point for broader and deeper research into the area between academia and related industrial bodies.

The aims of this work are as follows:

- To develop a classification of zircons based on metamictization level
- To assess the relationship between metamictization level and milling efficiency

* Corresponding author.
  E-mail address: mxs1126@alumni.bham.ac.uk (M.J. Smith).

- To visualise any impact of impurities on milling behaviour
- To assess the impact of heat treatment of zircon on milling behaviour

2. Literature survey

This section serves to identify and concisely summarise the key findings from the literature related to the topics presented in the main study.

Metamictization is a term used to describe the natural process by which the crystal structure of a mineral is destroyed by alpha radiation. The effects of metamictization on the properties of zircon have been discussed in the literature. With increasing radiation dose, hardness and density are known to decrease (Beirau, et al., 2016; Chakoumakos, et al., 1991; Murakami, et al., 1991), with hardness reducing by up to 48%, whilst fracture toughness has been shown to increase by 31.8% (Chakoumakos, et al., 1987). Refractive index and birefringence have also been shown to decrease (Vance and Anderson, 1972; Holland and Gottfried, 1955). X-Ray diffraction patterns broaden (Holland and Gottfried, 1955), and IR and Raman bands broaden linearly with increasing dose, with a corresponding decrease in intensities (Woodhead et al., 1991). Furthermore, cell parameters of zircon have been found to increase as a result of metamictization (Weber, 1990). These factors were considered when selecting the characterisation methods described in Section 3.2.

A review of the available literature for zircon milling identifies suitable lab-scale milling parameters and experimental methods (Gauna et al., 2017, Rendtorff et al., 2012), and it has been reported that intensive milling of crystalline zircon can itself amorphize the mineral to some extent (Gauna et al., 2018, Puclin and Kaczmarek, 1997). However, this phenomenon usually occurs with very fine materials milled at ultra-high intensities. In contrast, a Rietveld-RIR (reference intensity ratio) study by Damonte et al. (2017) investigated micronized zircon (D50 = 4 μm) and found that as well as a decrease in particle size, the amorphous content of zircon was in fact reduced by around 30% through milling to this size. Cell parameters remained unchanged, but no corresponding effect on key physical properties such as hardness, density or refractive index was discussed. Zircon which had experienced little to no natural radiation damage was utilised in this literature. These studies lack a discussion of how radiation effects specifically translate to the efficiency of the milling process via measurement of size reduction. While the literature indicates clearly that hardness and density of zircon are affected by metamictization, there is currently no indication of the corresponding impact on size reduction efficiency. As an energy-intensive process, knowledge of these effects for a given feed material is key in optimising milling efficiency. There is therefore a need to investigate the relationship between the level of metamictization, the particle size that can be achieved and the rate at which this occurs.

Throughput of lab-scale non-metamict zircon milling is addressed in the literature by measurement of the time required to achieve a desired particle size (Gauna et al., 2017). Comparisons can be drawn from the results of these studies to those that will be carried out for metamict

zircon, where similar particle size measurements are taken as a function of milling time in order to understand throughput for the process. Another study concluded that the hardness of zircon grains increases throughout milling (Topateş et al., 2020), which may result in decreased efficiency over time. This effect is to be anticipated, or otherwise compared, in the results of this paper.

3. Methods and materials

3.1. Materials

Six anonymised samples of zircon sand were provided by members of the Zircon Industry Association. These sands were sourced from various undisclosed locations across the globe in order to provide a representative range of metamictization levels. The exact sources and suppliers were not known to the investigators.

3.2. Characterisation of zircon samples – metamictization characteristics

In order to develop a classification of zircons based on the level of metamictization, several characterisation techniques were employed. These are summarised in Table 3.1.

The circularity, as an implication of sphericity (Liang, et al., 2016), of zircon grains (measured in ImageJ, using images acquired by SEM) and impurity content (EDX, as described above) were also measured to explain any non-metamictization effects observed in milling. All data was collated and used to determine a ranking of zircons based on their metamictization level.

One important observation from the above characterisation studies was that one of the provided samples had been previously calcined by the supplier. The impact of this on the milling behaviour is recognised in Section 4.

3.3. Milling methodology

The ideal media size for milling was calculated using Bond's Equation (1958). For the purpose of this calculation, work index was assumed constant at 20 kWh/sht across all sands (Michaud, 2015). This yielded an ideal media size of 17.8 mm; therefore, the closest commercially available size of 18 mm was selected. A suitable milling speed was identified by firstly using the ball mill critical speed equation (Dunne, 2019), above which collisions are minimal due to centrifugal forces. The critical speed was thereby calculated as 88.1 rpm. An optimal milling speed is suggested as 75 % of the critical speed (Michaud, 2015), yielding an ideal mill speed of 66 rpm.

The milling was carried out on a laboratory scale using a cylindrical ceramic vessel of internal diameter 230 mm and height 265 mm. For each sample, the vessel containing 18 mm diameter spherical alumina milling media and zircon sand was placed onto a roller mill (Glen Creston Ltd, UK).

A ball to powder mass ratio of 10:1 was selected as this is suitable for

Table 3.1
Characterisation Techniques for the Zircon Samples.

Experiment	Characteristic Measured	Equipment Used	Key parameters
Chemical Analysis (EDX)	Actinide (U, Th) Content	Philips XL-30 FEG ESEM	Sand grains mounted in resin, polished to 1 μm and surface gold-coated for conductivity
Helium Pycnometry	True Density	MicroMeritics AccuPyc II 1340 Gas Pycnometer	1 g sample size
X-Ray Diffraction	XRD Peak Intensity	Malvern Panalytical X-Ray Diffractometer	Range 5°-90°, fixed step size 0.003°, wavelength copper-K-alpha (1.5406 Ang), samples hand-ground to 10 μm and uniform PSD
Nitrogen Adsorption (BET)	Specific Surface Area	Micromeritics 3Flex Adsorption Analyzer	Vacuum created within sample chamber before purging with nitrogen
Scanning Electron Microscopy	Porosity and Surface Damage	Philips XL-30 FEG ESEM	Sand grains mounted in resin, polished to 1 μm and surface gold-coated for conductivity. Operated at 15 kV.

small scale dry milling (Suryanarayana, 2001). Therefore, masses of 5 kg and 500 g were selected for the media and sand sample respectively. The milling media were spherical alumina balls supplied by MinChem HMP Ltd (UK). The scope of this project specified dry milling of zircon in a rotary ball mill. A small amount of glycerol supplied by Sigma Aldrich was included in the mill to reduce the chance of particle coagulation.

At pre-selected intervals during the milling procedure, samples of powder were extracted from the mill for the purpose of particle size analysis. It was imperative that this sampling only took small amounts of zircon out of the mill such that milling behaviour was minimally affected by any change in total mass. Time intervals for sampling were set at one, two, four and eight hours in order to closely monitor early stage particle size reduction, which was expected to be pronounced. Further sampling was carried out at 24, 48 and 72 h in order to assess the long term milling behaviour and to locate the plateau at which maximum size reduction was achieved.

3.4. Determining particle size

Particle size distribution was measured by laser diffraction using a Mastersizer 2000 (Malvern Panalytical, UK), applying Mie theory. Flours were dispersed into a continuous flow of water with a small quantity of Dispex (BASF, USA). A material refractive index of 1.96 was used and obscuration was maintained in the range of 12–13%.

Particle size behaviour during milling is compared throughout Section 4. Differences in the shape of particle size distribution curves for one example of high-versus-low metamictization are evaluated in Section 4.2.5.

3.5. Thermal treatment

A furnace was used to anneal sands at a target temperature of 1000 K. Prior studies have shown that the effects of annealing zircon are significant after just 1 h of treatment (Zhang et al., 2000). However, it has been suggested that annealing of only a few hours may result in incomplete reaction (Nasdala et al., 2002). To ensure a complete reaction with comparable impact, a duration of 20 h was selected.

A ramp rate of 10 °C min^{-1} was set in order to achieve the target temperature. This temperature was maintained for 20 h before ramping down at 5 °C min^{-1}. The total duration of this procedure was 24 h. The gradual periods of temperature ramp up and ramp down were necessary in order to minimise the risk of thermal shock to the samples. Thermally treated samples were milled and compared to their untreated equivalent samples.

4. Results and discussion
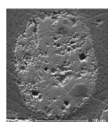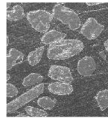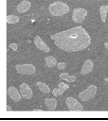
4.1. Characterisation results

Table 4.1 shows the ranking of metamictization determined by the characterisation steps summarised in Section 3.2. Some key measurement results are included. It should be noted that no characteristic data of zircon samples exhibited a linear trend, which is likely due to the impact of multiple factors on metamictization level. Samples were primarily categorised based on their measured physical characteristics, such as the density, in consistence with the literature. A previous study determined that zircon density may decrease to a value as low as 4160 kg m^{-3} as a result of metamictization (Murakami, et al., 1991), indicating that the samples in Table 4.1 may be limited in their range of metamictization level. However, the density of non-metamict zircon is typically reported in the literature within the range of 4600–4800 kg m^{-3} (Guo, et al., 2012). The measurements of density in Table 4.1 are consistent with this literature, both in terms of trend and the fact that the high metamict samples have a density below the expected minimum value, albeit not to the extent shown in the aforementioned study. The SEM imagery was used to corroborate the quantitative observations, with an abundance of physical defects indicating the expected softness of the high metamict samples.

The concentration of actinides found in samples was found to be generally consistent with the measured physical characteristics, albeit non-linear. This provided confidence in the concept of high levels of radioactivity, and therefore metamictization, causing physical changes in zircon. A related study suggested that zircon with up to 3100 ppm uranium was not considered highly metamict amongst all samples (Marsellos and Garver, 2010). Regarding this disagreement, it is proposed that the level of metamictization in zircon is not only a function of actinide content, but also the duration of the exposure. Since the geological age of each sample was unknown, it is reasonable to propose that Sample A, with a very high relative actinide content, would not necessarily exhibit extreme physical differences in comparison to samples with lower actinide content. It is clear that this is the case when comparing the true density of Sample A and Sample B. However, the surface area of Sample A was found to be much greater than that of Sample B. This could be explained by increased potential for surface damage in a softer sample, or indeed due to possible effects on surface morphology due to impurities, including the actinides (Hamouda et al., 2009).

Characteristic measurements that are unrelated to metamictization, namely impurity content and grain circularity, are also included in Table 4.1 for reference. A broad range of values were observed in both instances, with no distinct trend expected from literature.

As mentioned in Section 3.2, it was discovered during the study that

Table 4.1
Ranked Characteristic Propertird of the Six Zircon Samples.

Metamict Level	ID	U + Th (ppm)	True Density (kg m^{-3})	Surface Area (m^2 kg^{-1})	Typical SEM	Fe$_2$O$_3$ (%)	TiO$_2$ (%)	Al$_2$O$_3$ (%)	Average Grain Circularity
High	A	1039	4598	2388		0.19	1.10	0.80	0.55
	B	439	4594	719		0.04	0.25	1.60	0.41
Medium	C	467	4637	698		0.06	0.10	0.10	0.72
	D	474	4656	483		0.04	0.13	1.30	0.59
Low	E	311	4698	421		0.08	0.10	0.30	0.65
	F	355	4680	264		0.03	0.35	0.70	0.61

Sample F had been calcined by the zircon supplier. This explains the relatively low specific surface area measured for this sample; calcination is known to decrease the specific surface area of crystalline substances (Eder and Kramer, 2006; Volodin et al., 2017), which likely relates to the repair of surface defects.

4.2. Milling results

4.2.1. Preliminary particle sizing

The unmilled particle sizes for sands of interest are displayed in Table 4.2. These data serve as a reference point when comparing the size reduction behaviour over fixed periods of time. There is no apparent trend between the metamictization level of the unmilled sand and its particle size at this stage. This is the case for the fines, median and coarse sizing data. Although the sample size of six is too small to draw a meaningful conclusion, there is no available literature to suggest that a trend would be expected in this data.

4.2.2. Post-milling D_{50} particle size

In each of the following sections, the milling profile will be plotted with an accompanying plot of the reduction ratio, defined as the feed size divided by the product size. Fig. 4.1 shows the overall milling profile for each sand, with the accompanying reduction ratio plot in Fig. 4.2. This data focuses on the change in median particle size, D_{50}, over the duration of milling. In all cases, the D_{50} of the powder decreases with milling time, with the majority of the decrease occurring in the first 8 h of milling. A notable observation is that sample F exhibits a significantly different milling profile, concurrent with the knowledge that this sample had been previously calcined as part of the supply process. This observation highlights calcination processes as part of the zircon supply chain may yield significant benefits for those wishing to obtain a finer particle size. More generally, it is observed that the milling profiles of the samples, in terms of both size reduction and reduction ratio, do not provide a clear link to metamictization level throughout the full duration of milling.

In all cases, the theory that grain hardness increases throughout the milling process raised in the study of Topateş et al (2020) is supported, since the ability of particles to reduce in size worsens over time. Equally, this work provides advancement from the study of Gauna et al. (2017), where no significant change in D_{50} was achieved after 120 min of zircon milling treatment.

Distinct differences in milling efficiency between samples were observed in early stage milling (see Fig. 4.3). After just one hour of milling, Sample C (medium level of metamictization) had been ground to 4.6% of its original median size. In contrast, Sample B (high level of metamictization) reached a median size of 13.1% of its original size. While the margin for error on this data point is relatively large, the differences between initial milling efficiency remain large. From the median size profiles of sands between 0 and 8 h of milling, perhaps the most interesting observation is that both medium-metamict samples achieved smaller particle sizes than their high-metamict counterparts. However, the spread of data for low-metamict sands within this timeframe means that a trend between metamictization level and milling efficiency cannot be defined with a high degree of confidence at this stage.

Table 4.2
Unmilled Particle Sizing for the Zircon Samples.

Metamict Level	ID	D_{10} (µm)	D_{50} (µm)	D_{90} (µm)
High	A	80	112	157
	B	99	154	239
Medium	C	94	139	207
	D	89	157	262
Low	E	87	127	188
	F	92	150	240

As milling time progresses beyond 24 h, low-metamict samples continue to behave somewhat unpredictably. The data at 24 and 30 h hints that Sample E may be reaching a plateau above that of its higher metamict counterparts. Meanwhile, the earlier gap between high- and medium- metamict samples is maintained over this time period. From the 48-hour point, extensive milling has been completed for all samples, reflected by the plateau in particle size observed across the board. Interestingly, high- and medium-metamict samples appear to have reached a plateau by a similar point in time (24 h). The low metamict Sample E, however, exhibits a significant decrease in size between 30 and 48 h. It could be considered that there is a change in the mechanism of breakdown for particles in this timeframe, resulting in a double plateau. This occurred for both repeat trials of milling on the same sample. In ball milling of this kind, the primary grinding mechanism is expected to be predominantly impact grinding (Altun et al., 2021). However, the behaviour observed in sample E raises a theory that over an extended period, an alternative method – for example, attrition or shear-type mechanisms between finer particles – may begin to dominate.

Ultimately, there is a trend between metamictization level and D_{50} particle size after completion of 72 h of milling, as shown in Fig. 4.4. This data could suggest that low metamict sands could grind more readily due to their crystalline nature, while sharp fractures of high-metamict sands are less achievable due to their amorphous structure. However, there is contradiction more generally that a softer, high-metamict sand would require less energy to grind than a low-metamict sand whose hardness is retained. This behaviour raises the theory that high metamict zircon is soft but tough; these material properties might reduce the efficiency of grinding since brittle fracture is less likely. On the other hand, low metamict zircon is generally known to be harder, but may therefore exhibit brittle behaviour in milling, thus rendering fracture more likely. It should also be noted that while there is some clarity in trends after 72 h of milling, these are difficult to justify based on the lack of consistency in earlier stages of milling.

In addition to the comparisons between metamictization levels, it may be of interest to compare the differences in samples within the same assigned metamictization level. For the high metamict samples, there is a great difference in milling performance after 1 h, with Sample A achieving a reduction ratio of 15.3 in comparison to the 5.57 achieved by Sample B. This could relate to the relatively much larger surface area of Sample A (2388 m² kg⁻¹) than Sample B (719 m² kg⁻¹). This is indicative of a greater level of surface damage in the sample prior to milling, which in turn suggests that Sample A could be more easily broken down. This hypothesis relates to voidage at the sample surface rather than scratching, which is more indicative of hardness rather than ease of breakdown (Marghany, 2022).

In relation to this, it could be suggested that metamictization is not the major influencing parameter in milling performance, although it may have an indirect effect. Ultimately, the physical characteristics and mineralogy of a sample may have a more dominant effect, resulting in similar milling behaviour between high and low metamict samples in some instances. Limited data is available for the anonymised samples, but the importance of consistent ore characteristics in milling feed is well understood (Mkurazhizha, 2018). Beyond the early stage milling, the two high metamict samples (A and B) exhibit broadly similar reduction ratios. This is also true of the two medium metamict samples, C and D, particularly in the early stages of milling; the characteristic data for these samples (see Table 4.1) is much more alike than that of the high metamict samples. Comparisons between the low metamict samples are limited to the improved performance of Sample F due to its prior calcination.

4.2.3. Post-milling D_{10} particle size

Fig. 4.5 provides a visual comparison of the fines content, D_{10}, in each sample over the course of milling, with the accompanying reduction ratio plot in Fig. 4.6. Despite varying initial values of D_{10} (see
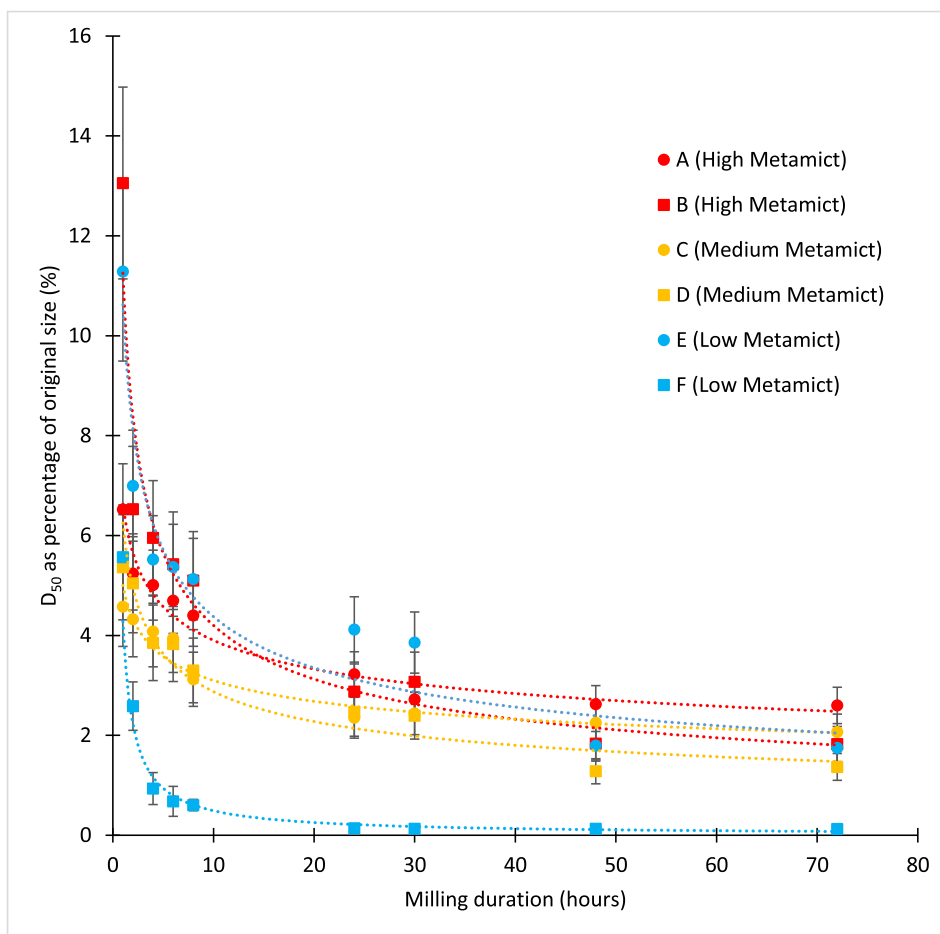
Fig. 4.1. D_{50} Particle Size Measured During Milling of the Three Pairs of Zircon Powders.

Table 4.2), most samples converge a similar value of between 0.6 and 0.8 μm after prolonged milling. The exception is sample F, whose behaviour can again be attributed to its prior calcination by the supplier. In contrast to the median size profiles, no distinct trend can be drawn between metamictization level and D_{10} particle size at 72 h. In fact, the milling profiles of sands in this figure are relatively similar with only minor deviations from one another. The most distinctive gap exists in the early stages of milling for sample B (high-metamict). For this sample, both D_{50} and D_{10} remain relatively high after one hour of milling, before conforming with the expected trend after two hours. This phenomenon was observed for multiple instances of size measurement for the sample and Dispex agent was used to reduce agglomeration of particles. It could be suggested that the metamict, and therefore less-brittle, nature of this sample is responsible for its initial resistance to grinding to a fine powder. Aside from initial difference, no distinct correlation can be drawn between the fines content throughout milling and metamictization level of zircon.

The concept that very fine zircon may become further amorphized by intense milling is introduced in the literature (Gauna et al., 2018, Puclin and Kaczmarek, 1997). There is little evidence to suggest that this occurred from the data in this study, although direct measurements of the amorphous content were not taken. In the case that this phenomenon did not occur for the fine D_{10} particles, it may be the case that the milling rate did not satisfy the requirement for ultra-intense grinding as discussed in the literature.

4.2.4. Post-milling D_{90} particle size

Fig. 4.7 indicates that, as with the data for D_{10}, there is no clear link between metamictization level and coarse particle grinding behaviour

for the samples in question during the early stages of milling. There is a wide and scattered spread of D_{90} across samples in this period. However, there is consistency between the median size data and D_{90} in terms of final particle size.

After 72 h of milling, it was observed that the higher the level of metamictization, the larger the value of D_{90} on average. Fig. 4.8 indicates that this could in fact represent a trend, with reduction ratio increasing as metamictization level reduces from high to medium to low at the 72 h mark. This indicates that the high metamict samples maintained a more significant percentage of larger coarse particles over the course of milling, and so milling performance overall was worse than low metamict sands. This behaviour links to the earlier mentioned hypothesis that lower metamict sands may fracture more easily due to their well-defined crystalline boundaries – they are likely to be more brittle than high metamict sands. Further studies could examine samples by microscopy after milling in order to determine the likelihood of this.

4.2.5. Particle size distribution curves

PSDs for Sample A (high metamict) and Sample E (low metamict) are displayed in Fig. 4.9 and Fig. 4.10 respectively; these were selected as representative examples of the observed trends.

The area under each curve represents the cumulative volume of particles within a given range of sizes. To the right of each figure, a pronounced, narrow PSD curve exists. This represents the original range of particle size found in the sample prior to milling. Moving left, the progression of particle size reduction over time can be observed. Upon commencement of milling, it was immediately clear that a broader PSD was produced due to the milling process. This is primarily driven by a small number of particles which grind very finely after only a very short
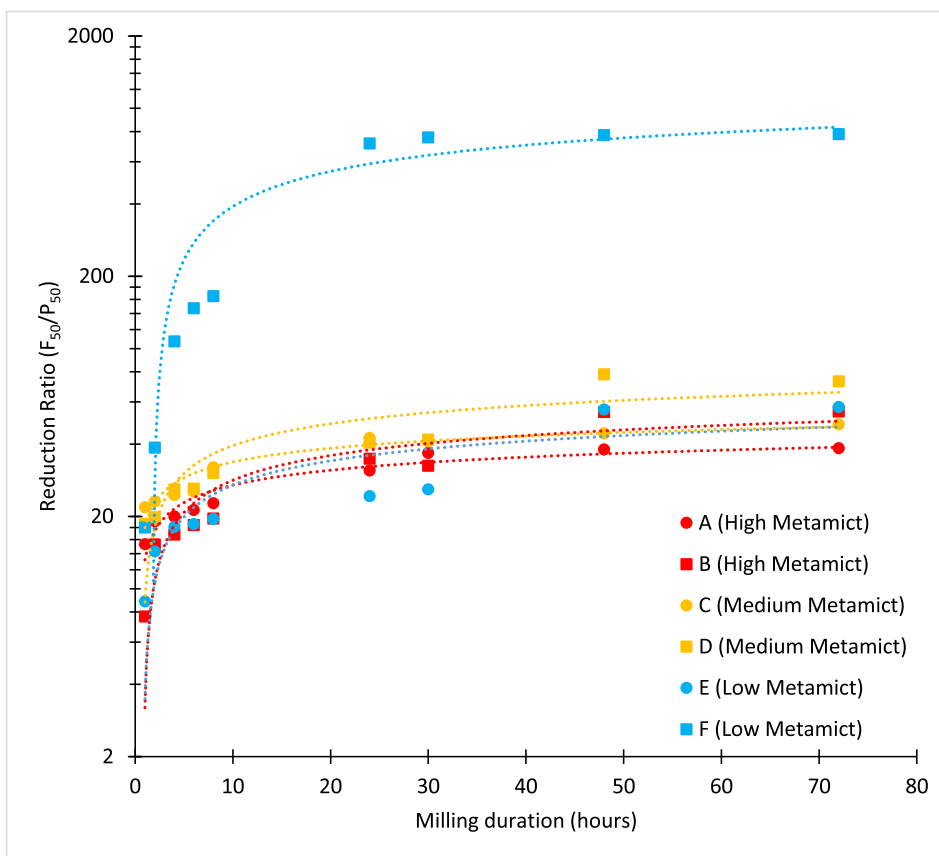
Fig. 4.2. D_{50} Reduction Ratio Measured During Milling of the Three Pairs of Zircon Powders.
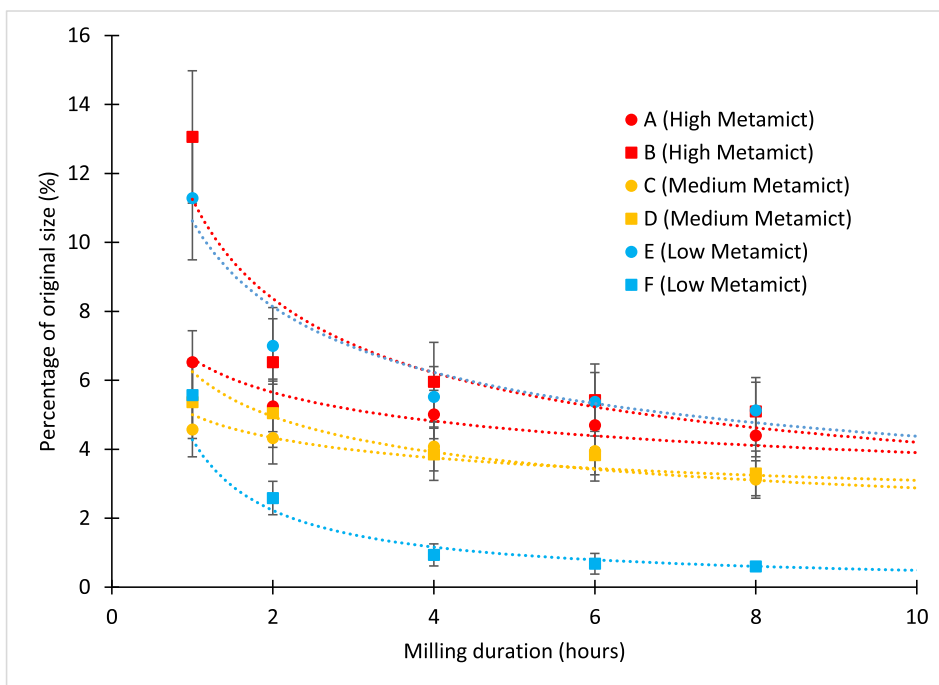

Fig. 4.3. D_{50} for initial eight hours of milling the six zircon powders.

milling duration. This can be visualised by the 'tail' on the left of each curve after 2 h of milling. After prolonged milling, this tail section of the curve is filled due to an increased in the number of fine particles and a more symmetrical PSD is achieved. From the data, it appears that high metamict samples achieve this level of symmetry at an earlier stage (24 h) than for low metamict samples (48 h). There is little deviation in the PSD for any milling time beyond this point.

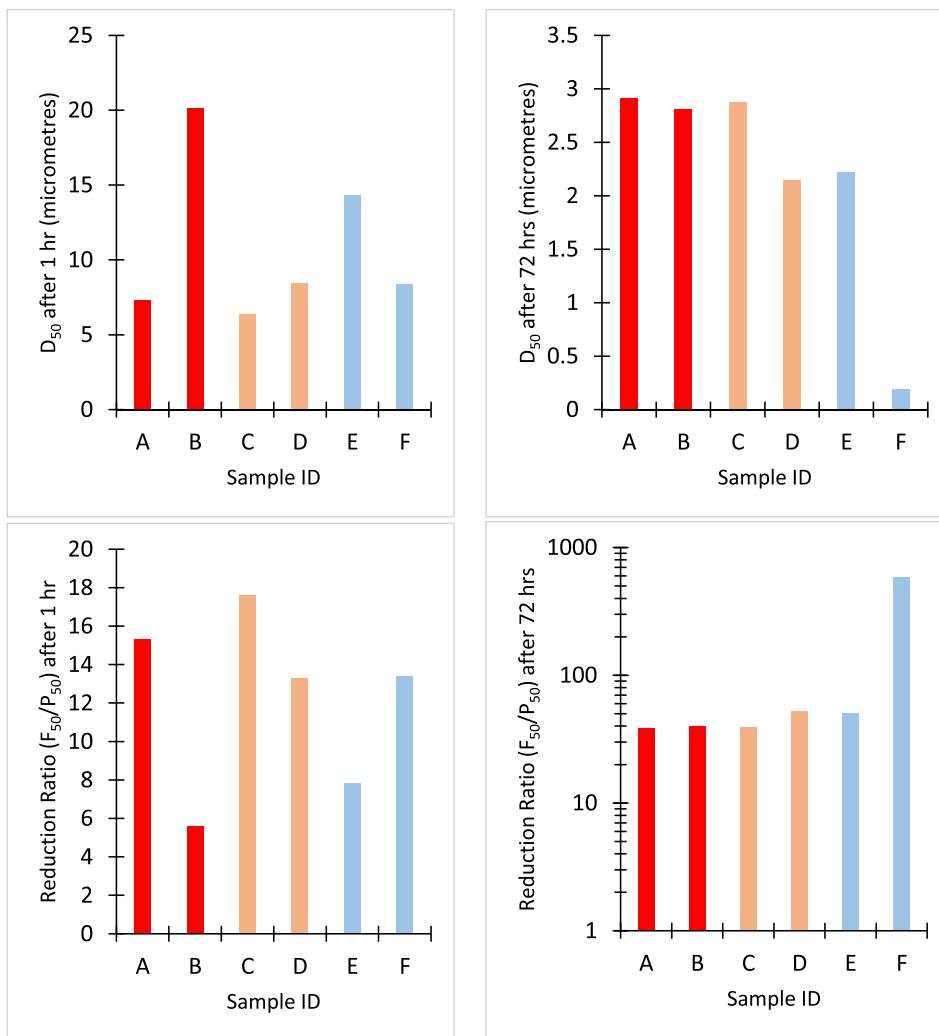Ultimately, the low metamict sample follows the classics stages of

Fig. 4.4. (a) Median Particle Size After 1 Hour and (b) After 72 Hours of Milling (c) Reduction Ratio After 1 Hour and (d) After 72 Hours of Milling.
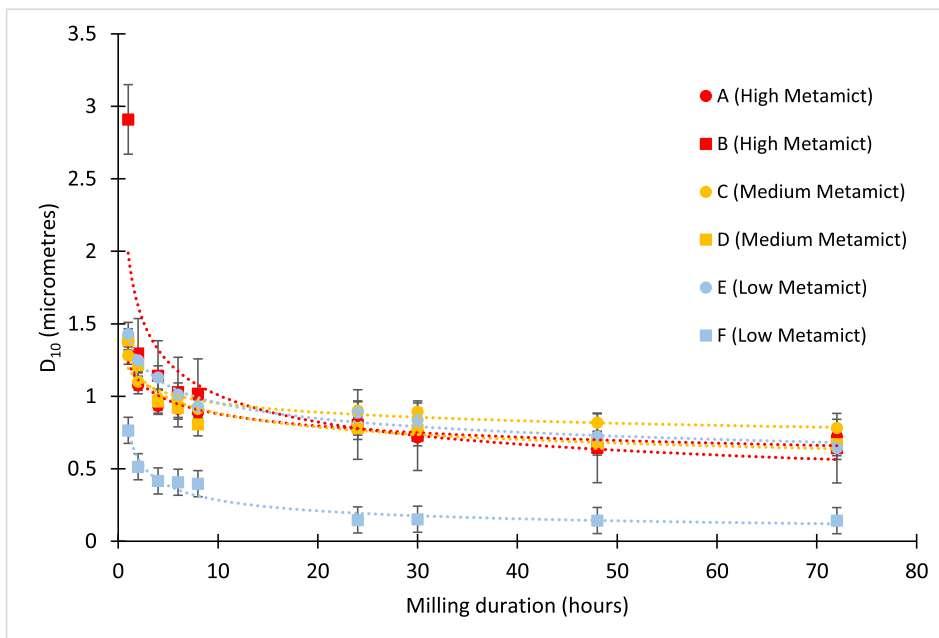

Fig. 4.5. D_{10} Particle Sizing of the Six Zircons Measured During Milling.
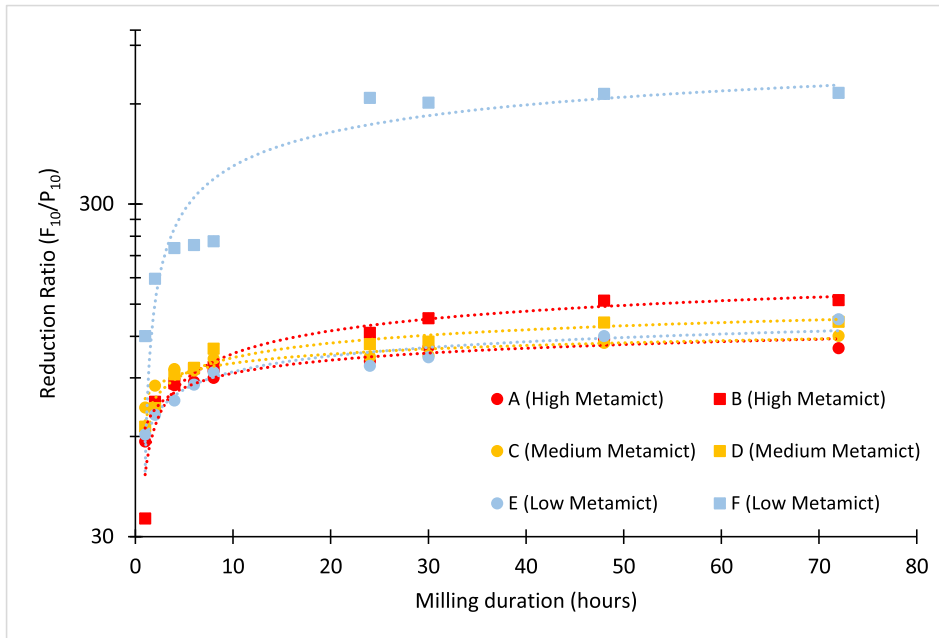
Fig. 4.6. D_{10} Reduction Ratio of the Six Zircons Measured During Milling.
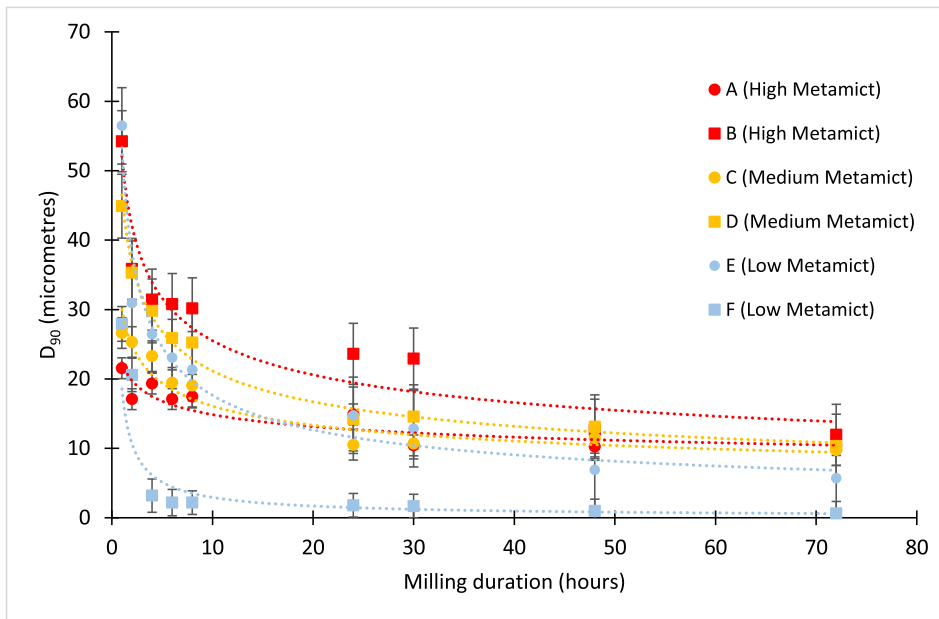

Fig. 4.7. D_{90} Particle Size of the Six Zircons Measured During Milling.

milling from monomodal to somewhat bimodal and then monomodal once more. The high metamict sample exhibits this to a slightly lesser extent, perhaps due to some greater degree of plastic deformation. The kurtosis (tail-heaviness) and skewness of each PSD was calculated and is shown in Table 4.3. Values of kurtosis above 3 indicate clustering of data within the peak of the curve (leptokurtic), while values below 3 indicate that data clusters mainly in the tails (platykurtic). Positive values of skewness indicate clustering of data towards lower values of particle size, while clustering at higher particle size is reflected by a negative value of skewness.

Initially, both samples exhibit a distribution with kurtosis close to that of the normal distribution (mesokurtic, kurtosis value = 3). Samples are moderately positively skewed, meaning that there is clustering towards the finer particle sizes. As milling duration increases, both

samples exhibit an increase in both kurtosis and skewness. The high metamict sample, A, demonstrates these changes to a stronger extent than the low metamict sample, E. Ultimately, this means that there is an increased skew, on average, towards finer particle ranges in both samples, as well as an increased tendency for particle sizes close to the mean. When considering skewness and kurtosis, it should be noted that the x-axis scale used in Fig. 4.9 and Fig. 4.10 is logarithmic.

The fracture behaviour observed from the PSD for the low metamict sample E is reflective of a hard, brittle sample. In contrast, the PSD of the high metamict sample, A, suggests that the sample is softer but tougher. This is deduced from the knowledge that crystalline materials typically exhibit brittle fracture due to well-defined planes within the structure, whereas non-crystalline materials are more likely to break down through ductile fracture (Haldar and Tišljar, 2014; Ding, et al., 2015).
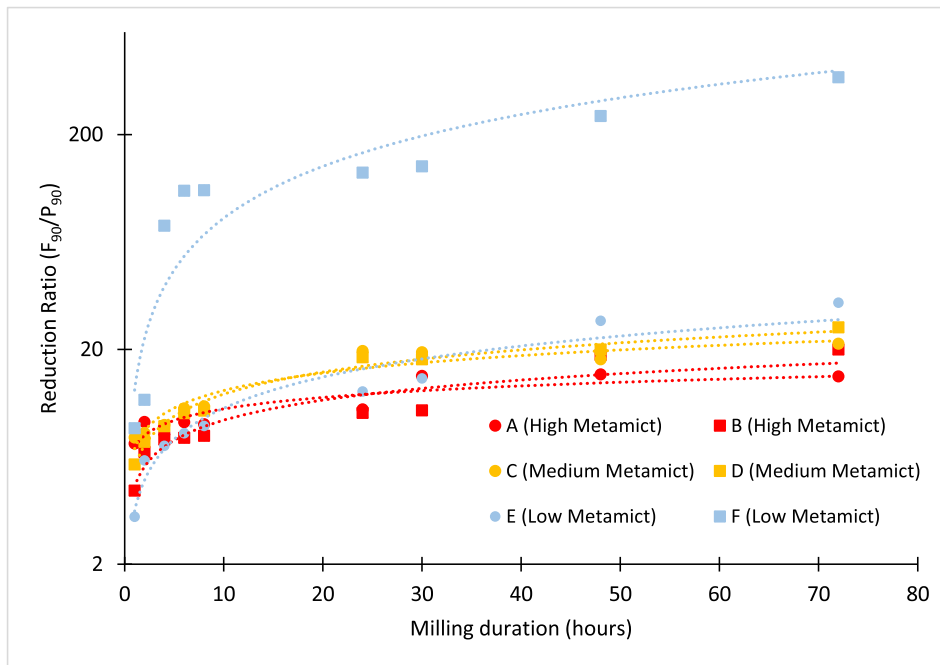
Fig. 4.8. D_{90} Reduction Ratio of the Six Zircons Measured During Milling.
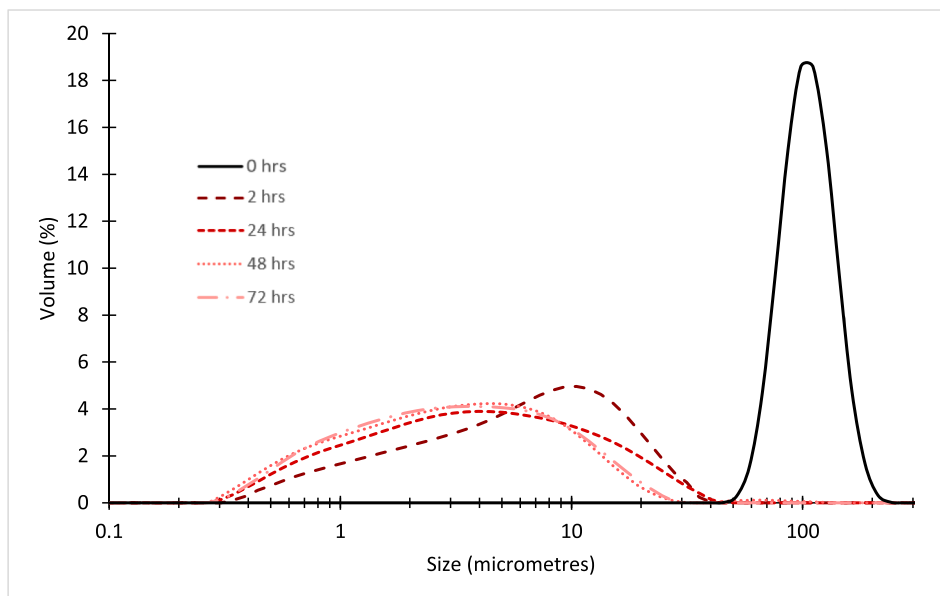

Fig. 4.9. PSDs for Sample A - High Metamict Zircon.

The final PSDs generated for low and high metamict samples are distinctly different in shape. The high metamict sample exhibits a broader curve than that of the low metamict sample. This indicates that a wider range of particle sizes exist in the final milled sample for high metamict zircon flour. This supports the fracture mechanisms described; a greater proportion of coarse particles remain after milling the high metamict sample, since amorphous materials typically produce irregular and elongated fragments when broken down due to deformation in the period leading up to the fracture (Eyres and Bruce, 2012; LibreTexts, 2022). In contrast, the relatively narrower peak of the low metamict sample reflects a smaller overall span of particle size, where the lesser extent of PSD broadening indicates minimal particle deformation and so brittle crystalline fracture. This may be crucial information when determining suitability of zircons for their end-product application,

specifically where a certain particle size is necessary. Low metamict sands appear to offer a consistent, refined range of particle size without the need for additional sieving steps. High metamict zircon flours may pose an issue in applications where particle size must be strictly adhered to.

4.2.6. Comparison of characterisation data with milling behaviour

Figs. 4.11 and 4.12 are included for comparison of the metamictization level of samples against their final particle size, but also for a more detailed view of the impact of specific physical characteristics of zircon.

High, medium, and low metamict samples are highlighted in red, orange, and blue respectively for consistency with previous sections. Fig. 4.11(a) shows the relationship between XRD maxima of samples
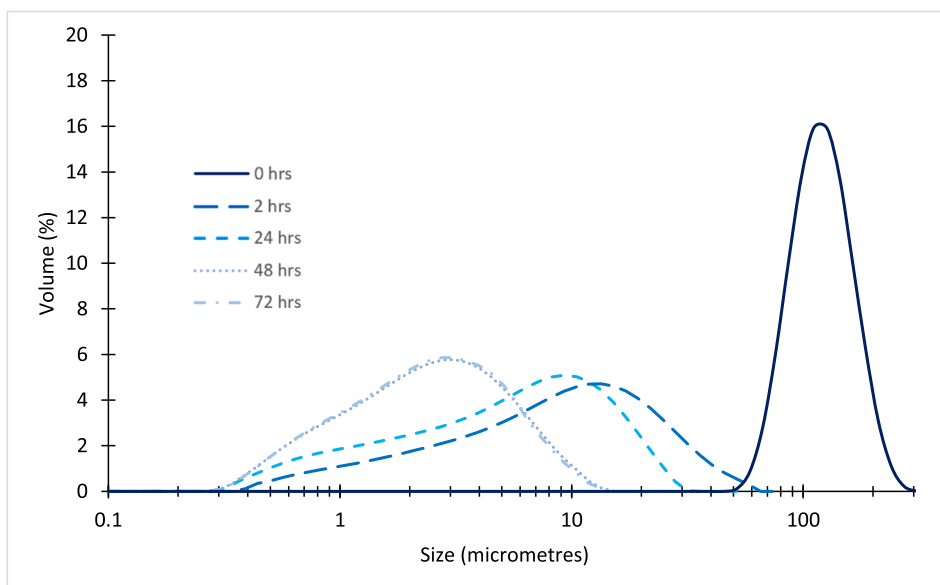
Fig. 4.10. PSDs for Sample E - Low Metamict Zircon.

Table 4.3
Kurtosis and Skewness of PSDs.

Sample ID	Prior to milling		After 72 h of milling	
	Kurtosis	Skewness	Kurtosis	Skewness
A (high metamict)	3.43	0.68	5.87	1.67
E (low metamict)	3.51	0.77	4.80	1.32

read at 53° (selected as an expected peak in zircon), and the final particle size after 72 h of milling. The data for the calcined sample F is interesting to return to at this point, primarily because there is limited evidence in the characterisation data that this sample had been previously treated. This became truly apparent only upon commencement of milling studies, where milling efficiency was observed to be significantly better through effective particle size reduction. In terms of trend analysis, therefore, that data for sample F may be disregarded in this section since its prior calcination gives the sample outlier status in terms of particle size. From the relevant data, a weak negative trend may be assumed between XRD peak intensity and particle size. This is consistent with the observation that low metamict samples reach a marginally smaller particle size than higher metamict zircon; XRD intensity and metamictization level are closely linked. Comparing between samples of the same metamictization level yields a potentially interesting result. For each pair of samples within the same damage level, the one with the lesser XRD peak intensity presents the lower final particle size of the two. While this may be an interesting sub-trend, it should not discredit the expected logical trend seen in the overall data.

Similar conclusions can be drawn from the density data when compared to final particle size. There is again the expected negative progression due to the interlinking relationships between metamictization level, density and milling performance. However, comparison within each level here offers no specific trend. In contrast, Fig. 4.11(c) indicates that there may be some positive relationship between the specific surface area of each sample and the level of metamictization, albeit with a plateau at the higher end of metamictization. Fig. 4.11(d) shows particle size data plotted against the circularity characterisation data. This data is very well dispersed, and no strong relationships can be identified in this case. One interesting data point is that of sample B. This links to the observation that this sample was found to have relatively low circularity of grains (0.41) compared to other samples. This could be the cause of the initially high D_{50} observed for sample B after one hour of

milling; a link may be identified between irregular particle shape and efficiency of particle size reduction. Since sample B ultimately converged to a similar milling profile to other samples, it may be the case that irregular shaped particles tended to wear down by attrition into more circular ones. Further work could investigate more closely the effect of particle shape on grinding behaviour.

It holds true that none of the above data suggests that there is a significant strong relationship between the measured characteristics and final particle size obtained through milling, with the potential exception being the influence of surface area. This may be explained by an increased specific surface area offering greater availability of sites for abrasive contact between zircon sand particles during the milling process. Metamictization leads to a defect population which in turn leads to a higher surface area, and might also reduce strength as per the Griffith relation (Sun and Jin, 2012).

An objective of this paper was to ensure that the impact of impurities (present in the original samples) on milling was assessed alongside any metamictization effects. In Fig. 4.12, it is therefore useful to compare the impurity content of samples within the same metamictization level. Samples were selected with this intended comparison in mind. It was observed that within each level of metamictization (illustrated by the colour scheme), samples with greater alumina content reached a finer particle size than those with lower alumina content. The data as a whole does not match any such trend, which raises uncertainty about any true impact of alumina content on milling performance. The same argument can be made for iron oxide content, where there is a consistent trend within each level of metamictization, but great dispersion of data overall. Ultimately, there appears to be little impact of impurities on milling across samples, with the exception of the anomalous sample.

4.2.7. Effect of heat treatment

Fig. 4.13 details the milling behaviour of samples after thermal treatment in comparison to the same sample milled without any treatment. The overwhelming conclusion that can be drawn from this study is that the process of heat treatment resulted in a less rapid and ultimately less efficient milling process. The initial rate of particle size reduction was significantly less for all samples. Furthermore, it appears that the plateau of final particle size was achieved at a size approximately four times larger than that of an untreated zircon sample. These features could be explained by the restored crystallinity, and therefore hardness, of zircon samples due to heat treatment; this transition was previously demonstrated by Zhang et al. (2000). Where samples exhibited varying
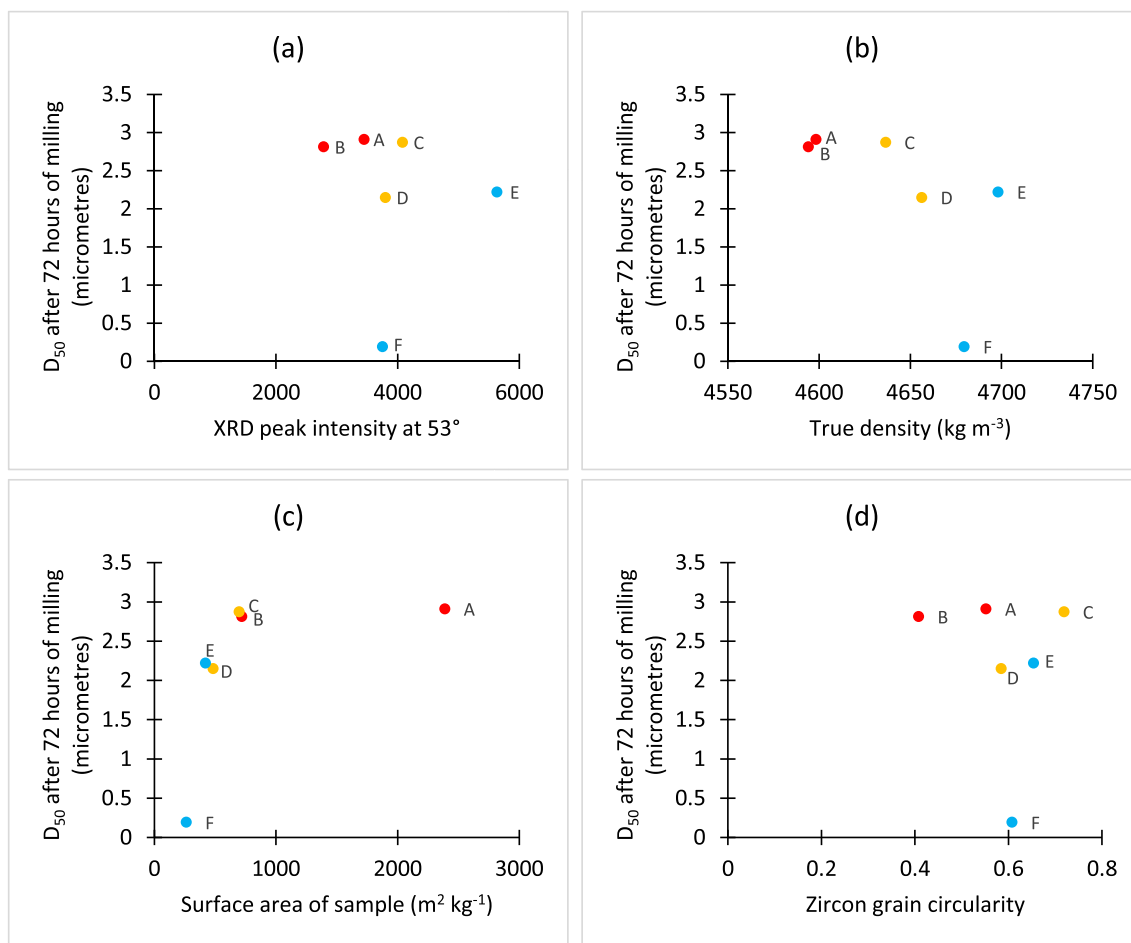
Fig. 4.11. Comparison of Final Particle Size Against (a) XRD Peak Intensity (b) Density (c) Pre-Milled Surface Area and (d) Grain Circularity of Zircon.
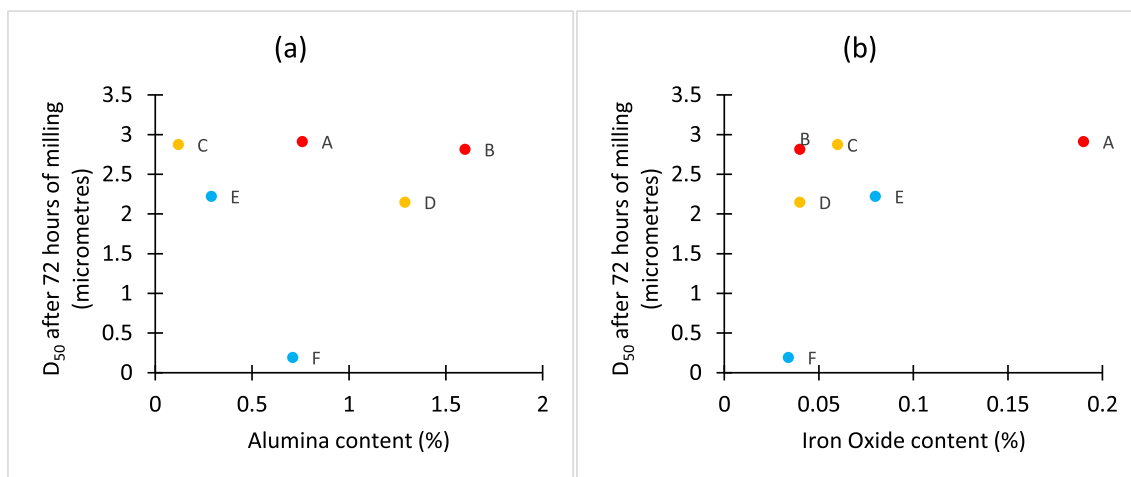

Fig. 4.12. Comparison of Final Particle Size with (a) Alumina and (b) Iron Oxide Impurity Content in Zircon.

milling profiles in early stage milling, it was observed that there was some level of standardisation in milling due to thermal treatment during this stage. However, it is difficult to assess this standardisation for later stage milling due to the similarity in milling profiles of untreated samples beyond the 24-hour mark.

Interestingly, the behaviour of these samples following heat treatment is distinctly different to the milling behaviour observed by the calcined sample F in earlier sections. While these samples were not as easily milled following treatment, sample F readily achieved a fine

particle size after short term milling. This indicates that the heat treatment procedure utilised here was different to the calcination process carried out by the supplier on sample F. The procedures in this study utilised a temperature of 1000 K, which is close to the sintering temperature of pure zircon. As a result, microcracks and defects within the structure may have repaired to some extent, alongside the restoration of crystallisation. There is a need to further understand the mechanisms of change in zircon structure throughout both procedures.

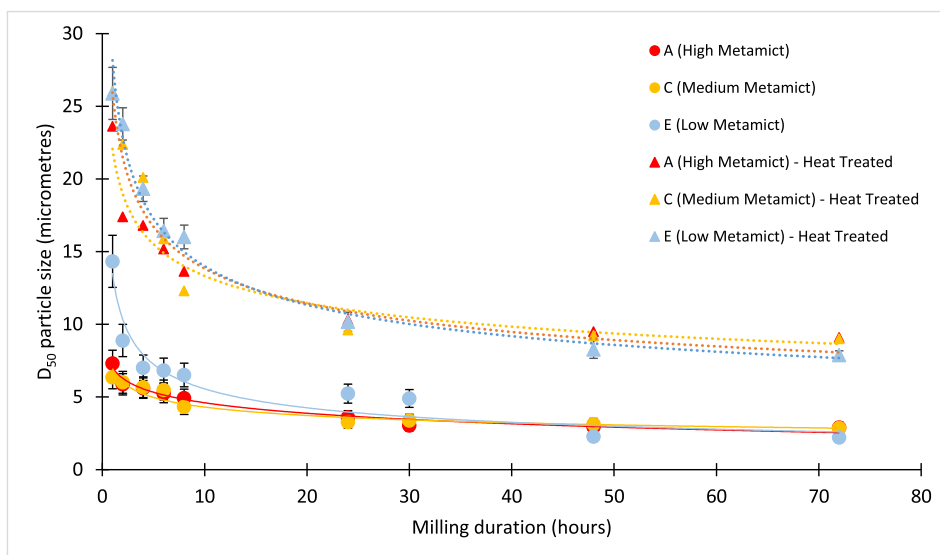Perhaps most notable is the fact that all samples demonstrated a shift

Fig. 4.13. D_{50} Particle Sizing of the Six Heat-Treated Zircons Measured During Milling.

in their milling profile due to thermal treatment, regardless of their initial level of metamictization. This might suggest that all zircons in the sample were, to some extent, damaged by radiation. It is highly likely that this is true, since all samples contained a measurable quantity of actinides.

4.3. Future recommendations

It is important to note that the range of sands tested in this study were representative of those that are commercially available. This primarily means that a limited range of actinide content was observed across samples, typically between 350 and 500 ppm, with the exception of sample A. More extreme cases of high or low actinide content and therefore metamictization in zircon will exist, and indeed may have a more notable impact on milling behaviour. These types of zircon may in future become more industrially relevant; future work may wish to expand the scope of this study to include such zircon types. It is suggested that metamictization level could be characterised further through calculation of the ratio of decay products to parent actinides. Furthermore, exploration of the impact of metamictization on downstream product quality properties would be industrially useful. This type of investigation should encompass factors beyond U and Th concentrations, particularly initial hardness and colour. Similarly, future investigations could assess the amorphous content of sample after they have been milled to corroborate the work of Gauna et al., (2018), Puclin and Kaczmarek, (1997) and Damonte et al. (2017).

The laboratory scale experimentation in this study provides a good foundation for understanding zircon milling behaviour. It is unlikely, however, that a 72 h milling duration would be practical on an industrial scale due to the energy requirements. In order to more accurately predict the behaviour of metamict zircons in milling, larger scale experimentation would be a logical next step. A larger vessel and closer mapping of practices to those used industrially would provide a clearer picture of adaptations that could be made to milling processes on an industrial scale to suit the quality of feed material. It is recommended that larger scale studies could illustrate power measurements in addition to particle size data, since energy requirements in a small study without scale-up are less relevant to the zircon industry.

Furthermore, the use of glycerol as a grinding aid in this study was effective, although a small level of particle coating on the milling media was observed after 72 h. In order to minimise particle coagulation after prolonged grinding, future research would benefit from a study into the optimum ratio of glycerol to zircon feed material.

Additionally, the heat treatment study could be expanded to explore a range of temperatures and durations, and investigation into the calcining procedures used for sample F could be carried out. This could be used to determine any optimum parameters that could be selected to balance overall product quality with milling efficiency.

5. Conclusion

This study has yielded some intriguing findings regarding the effects of metamictization on the physical and chemical properties of zircon, and the subsequent milling behaviour that was observed. The characterisation of samples undoubtedly allowed for inference of relative metamictization level in zircon samples based on a range of experimental data. However, the relationship between each measured characteristic was found not to be strictly linear. A true comparative ranking of metamictization levels is therefore difficult to define among zircons with similar actinide content. It may be the case that the characteristics of zircon samples are impacted to a varying extent dependent on additional external factors that were not considered in this study, for example the geological age of the sample or any natural annealing processes it may have been exposed to over its lifetime. The nature of the metamictization as a geological process inevitably facilitates variation in the overall change observed.

Despite this, some relationships can be drawn between the expected level of metamictization in a sample and its milling behaviour. Highly metamict zircons were found to exhibit a much broader particle size distribution after extensive milling compared to that of less metamict zircon samples. Furthermore, a marginally smaller average particle size, D_{50}, was attainable for low metamict zircons.

Thermal treatment of zircon was deemed to have a significant effect on milling behaviour for samples across all levels of metamictization. Specifically, the milling process was shown to be less efficient for heat-treated samples compared to the process for the same sample left untreated. This behaviour may be attributed to the hardness restored in the zircon through reversal of metamictization. While restoration of the crystalline structure of zircon through thermal treatment may be beneficial in terms of end product characteristics, such as refractive index and hardness, these improvements should be assessed against the reduced efficiency of grinding that arises. Furthermore, the difference between annealed and non-annealed milling behaviour was not observed to vary greatly as a function of metamictization.

The above findings are relevant to industrial applications where precise ranges of zircon particle size are required for the desired

application. Low metamict samples were found to be most suitable for this, but as high metamict sands increase in natural prevalence, industrial millers may need to consider additional sieving steps to reduce the variation in milled particle size observed in high metamict zircon.

CRediT authorship contribution statement

M. Smith: Investigation, Writing – original draft, Writing – review & editing. **E. Jones:** Writing – review & editing. **S. Blackburn:** Writing – review & editing. **R.W. Greenwood:** Writing – review & editing.

Declaration of Competing Interest

The authors declare the following financial interests/personal relationships which may be considered as potential competing interests: Matthew Smith reports financial support was provided by Zircon Industry Association.

Data availability

The authors do not have permission to share data.

Acknowledgements

References

Altun, O., Sahin, O., Toprak, A., 2021. Effects of impact and attrition mechanisms on size distribution and liberation characteristics of the components. Advanced Powder Technology 32 (10), 3550–3563.

Beirau, T., Nix, W., Bismayer, U., Boatner, L., Isaacson, S., Ewing, R., 2016. Anisotropic mechanical properties of zircon and the effect of radiation damage. Phys Chem Minerals 43, 627–638.

BOND, F. C., 1958. Ball size selection. Mining Engineering. Trans. AIME 592-595.

Chakoumakos, B., Lumpkin, G., Ewing, R., 1991. Hardness and elastic modulus of zircon as a function of heavy-particle irradiation dose: I. In situ α-decay event damage. Radiation Effects and Defects in Solids 118, 393–403.

Chakoumakos, B.C., Murakami, T., Lumpkin, G.R., Ewing, R.C., 1987. Alpha-Decay–Induced Fracturing in Zircon: The Transition from the Crystalline to the Metamict State. Science 236 (4808), 1556–1559.

Damonte, L.C., Rivas, P.C., Pasquevich, A.F., Andreola, F., Bondioli, F., Ferrari, A.M., Tositti, L., Cinelli, G., 2017. Structural Characterization of Natural and Processed Zircons with X-Rays and Nuclear Techniques. Advances in Condensed Matter Physics 2017, 1–9.

Ding, B., Li, X., Zhang, X., Wu, H., Xu, Z., Gao, H., 2015. Brittle versus ductile fracture mechanism transition in amorphous lithiated silicon: From intrinsic nanoscale cavitation to shear banding. Nano Energy 18, 89–96.

DUNNE, R., KAWATRA, S., YOUNG, C., 2019. SME Mineral Processing and Extractive Metallurgy Handbook.

Eder, D., Kramer, R., 2006. Impedance spectroscopy of reduced monoclinic zirconia. Physical Chemistry Chemical Physics 8 (38), 4476–4483.

Eyres, D., Bruce, G., 2012. 8 - Stresses to which a ship is subject. Ship Construction 7, 67–78.

Gauna, M., Conconci, S., Suarez, G., Aglietti, E., Rendtorff, N., 2018. Dense Zircon (zrsio4) Ceramics by a Simple Milling-Sintering Route. Science of Sintering 50, 15–28.

Gauna, m., rendtorff, n; conconci, s; suarez, g; pasquevich, a; rivas, p; damonte, l,, 2017. Fine zircon (zrsio4) powder mechanical activation, a Perturbed Angular Correlation (PAC) analysis. Ceramics International 43, 11929.

GUO, S., CHEN, B., DURRANI, S. 2012. Chapter 4 – Solid-State Nuclear Track Detectors. Handbook of Radioactivity Analysis, 3: 233-298.

HALDAR, S., TIŠLJAR, J., 2014. Chapter 2 – Basic Mineralogy. Introduction to Mineralogy and Petrology, 1: 39-79.

Hamouda, A., Stasevich, T., Pimpinelli, A., Einstein, T., 2009. Effects of impurities on surface morphology: some examples. Journal of Physics: Condensed Matter 21 (8), 084215.

Holland, H., Gottfried, D., 1955. The effect of nuclear radiation on the structure of zircon. Acta Crystallographica 8 (6), 291–300.

Liang, F., Sayed, M., Al-Muntasheri, G., Chang, F., Li, L., 2016. A comprehensive review on proppant technologies. Petroleum 2, 26–39.

LIBRETEXTS, 2022. Crystalline and Amorphous Solids. Available at: https://chem.libretexts.org/@go/page/6402.

Marghany, m., 2022. An introduction to minerals, rocks and mineral deposits. Advanced Algorithms for Mineral and Hydrocarbon Exploration Using Synthetic Aperture Radar 1, 1–30.

Marsellos, A., Garver, J., 2010. American Mineralogist 95, 1192–1201.

MICHAUD, L. 2015. Top Ball Size of Grinding Media - Fred C Bond Equation and Method. 911 Metallurgist. www.911metallurgist.com/blog/top-ball-size-grinding-media-calculator.

MKURAZHIZHA, H. 2018. The effects of ore blending on comminution behaviour and product quality in a grinding circuit – Svappavaara (LKAB) Case Study. Minerals and Metallurgical Engineering - Lulea University of Technology.

Murakami, T., Chakoumakos, B., Ewing, R., Lumpkin, G., Weber, W., 1991. Alpha-Decay Event Damage in Zircon. American Mineralogist 76, 1510–1532.

Nasdala, L., Lengauer, C., Hanchar, J., Kronz, A., Wirth, R., Blanc, P., Kennedy, A., Seydoux-Guillaume, A., 2002. Annealing radiation damage and the recovery of cathodoluminescence. Chemical Geology 191 (1–3), 121–140.

Puclin, T., Kaczmarek, W.A., 1997. A high temperature X-ray diffraction study of the crystallisation of amorphous ball-milled zircon. Colloids and Surfaces 129–130.

Rendtorff, N., Grasso, S., Hu, C., Suarez, G., Aglietti, E., Sakka, Y., 2012. Dense zircon (zrsio4) ceramics by high energy ball milling and spark plasma sintering. Ceramics International 38, 1793–1799.

SUN, C. T., JIN, Z. H., 2012. Chapter 2 – Griffith Theory of Fracture. Fracture Mechanics, 1, 11-24.

Suryanarayana, c.,, 2001. Mechanical Alloying and Milling. Progress in Materials Science 46, 1–184.

Topateş, G., Alici, B., Tarhan, B., Tarhan, M., 2020. The effect of zircon particle size on the surface properties of sanitaryware glaze. Materials Research Express 7, 1–9.

Vance, E.R., Anderson, B.W., 1972. Study of metamict Ceylon zircons. Mineralogical Magazine 38 (197), 605–613.

Volodin, A., Bedilo, A., Stoyanovskii, V., Zaikovskii, V., Kenzhin, R., Mishakov, I., Vedyagin, A., 2017. RSC Advances 7, 54852.

Weber, w. j., 1990. Radiation-induced defects and amorphization in zircon. Journal of Materials Research 5 (11), 2687–2697.

Woodhead, J., Rossman, G., Silver, L., 1991. The metamictization of zircon: Radiation dose-dependent structural characteristics. American Mineralogist 76 (1–2), 74–82.

Zhang, M., Salje, E., Capitani, G.C., Leroux, H., Clark, A., Schluter, J., Ewing, R., 2000. Annealing of α-decay damage in zircon: a Raman spectroscopic study. Journal of Physics: Condensed Matter 12, 3131–3148.

Zircon industry association, 2015. Technical handbook on zirconium and zirconium compounds. ZIA. www.zircon-association.org/download-handbook.html, London.